HHS Public Access

Author manuscript

Neuromodulation. Author manuscript; available in PMC 2024 July 01.

Published in final edited form as:

Neuromodulation. 2023 July ; 26(5): 938–949. doi:10.1016/j.neurom.2023.03.006.

Spinal Cord Stimulation Increases Chemoefficacy and Prevents Paclitaxel-Induced Pain via CX3CL1

Eellan Sivanesan, MD[1], **Karla R. Sanchez, PhD**[1], **Chi Zhang, PhD**[1], **Shao-Qiu He, PhD**[1], **Bengt Linderoth, MD, PhD**[2], **Kimberly E. Stephens, PhD**[3,4], **Srinivasa N. Raja, MBBS**[1], **Yun Guan, PhD, MD**[1,5]

[1]Department of Anesthesiology and Critical Care Medicine, School of Medicine, Johns Hopkins University, Baltimore, MD, USA

[2]Department of Clinical Neuroscience, Karolinska Institute, Stockholm, Sweden

[3]Department of Pediatrics, University of Arkansas for Medical Sciences, Little Rock, AR, USA

[4]Arkansas Children's Research Institute, Little Rock, AR, USA

[5]Department of Neurological Surgery, School of Medicine, Johns Hopkins University, Baltimore, MD, USA

Abstract

Introduction: Despite increasing utilization of spinal cord stimulation (SCS), its effects on chemoefficacy, cancer progression, and chemotherapy-induced peripheral neuropathy (CIPN) pain remain unclear. Up to 30% of adults who are cancer survivors may suffer from CIPN, and there are currently no effective preventative treatments.

Materials and Methods: Through a combination of bioluminescent imaging, behavioral, biochemical, and immunohistochemical approaches, we investigated the role of SCS and paclitaxel (PTX) on tumor growth and PTX-induced peripheral neuropathy (PIPN) pain development in T-cell–deficient male rats (Crl:NIH-*Foxn1*^{rnu}) with xenograft human non–small cell lung cancer. We hypothesized that SCS can prevent CIPN pain and enhance chemoefficacy partially by modulating macrophages, fractalkine (CX3CL1), and inflammatory cytokines.

Address correspondence to: Eellan Sivanesan, MD, Department of Anesthesiology and Critical Care Medicine, School of Medicine, Johns Hopkins University, 460D Phipps Bldg, 600 N Wolfe St, Baltimore, MD 21287, USA. esivane1@jh.edu.

Authorship Statements

Eellan Sivanesan conceptualized and designed the study. Eellan Sivanesan, Karla R. Sanchez, Chi Zhang, and Shao-Qiu He conducted or assisted with experiments. Eellan Sivanesan analyzed and visualized the results. Eellan Sivanesan also conducted the project administration and supervision, and wrote the first draft. Eellan Sivanesan and Yun Guan wrote the second draft. Eellan Sivanesan, Yun Guan, Kimberly E. Stephens, Srinivasa N. Raja, and Bengt Linderoth provided critical intellectual revision of the manuscript. All authors read and approved the final manuscript.

SUPPLEMENTARY DATA

To access the supplementary material accompanying this article, visit the online version of *Neuromodulation: Technology at the Neural Interface* at www.neuromodulationjournal.org and at https://doi.org/10.1016/j.neurom.2023.03.006.

Conflict of Interest: Eellan Sivanesan, Karla R. Sanchez, Chi Zhang, Shao-Qiu He, and Kimberly E. Stephens reported no conflict of interest. Bengt Linderoth is a consultant for Elekta AB. Srinivasa N. Raja is a consultant for AbbVie, Averitas Pharma, Bayer, and Lexicon Pharmaceuticals. Yun Guan and Srinivasa N. Raja are principal and coinvestigators in a research grant from Medtronic, Inc. Yun Guan received a research award from TissueTech, Inc.

Results: We show that preemptive SCS enhanced the antitumor efficacy of PTX and prevented PIPN pain. Without SCS, rats with and without tumors developed robust PIPN pain-related mechanical hypersensitivity, but only those with tumors developed cold hypersensitivity, suggesting T-cell dependence for different PIPN pain modalities. SCS increased soluble CX3CL1 and macrophages and decreased neuronal and nonneuronal insoluble CX3CL1 expression and inflammation in dorsal root ganglia.

Conclusion: Collectively, our findings suggest that preemptive SCS is a promising strategy to increase chemoefficacy and prevent PIPN pain via CX3CL1-macrophage modulation.

Keywords

Chemotherapy; chronic pain; non–small cell lung cancer; peripheral neuropathies; spinal cord stimulation

INTRODUCTION

Although chemotherapy-induced peripheral neuropathy (CIPN) greatly affects quality of life and can limit cancer treatment options, no drugs have been approved by the US Food and Drug Administration to prevent or treat it. Paclitaxel (PTX) is a taxane analog used to treat solid tumors, including non–small cell lung cancer (NSCLC). Its neurotoxicity can cause somatosensory aberrations and debilitating pain, classically presenting in a stocking-and-glove distribution.[1] In addition to persistent symptoms in survivors of cancer, CIPN can force dose reductions during chemotherapy treatment and compromise remission rates.[2]

Spinal cord stimulation (SCS) is used to alleviate certain refractory pain conditions. Although clinical reports of SCS (months after chemotherapy) for treatment of established CIPN pain[3,4] and our report of early neuromodulation for prevention and treatment of herpes zoster-associated pain[5] are promising, there is a paucity of literature on the application of early or preemptive SCS (ie, SCS before or during injury) to prevent CIPN. Although objective diagnostic criteria are lacking, PTX-induced peripheral neuropathy (PIPN) is often associated with recruitment of innate immune cells such as macrophages, monocytes, and neutrophils to dorsal root ganglia (DRG) that contain the primary sensory neurons.[6,7] Relatedly, our previous study revealed that early SCS upregulates spinal cord gene networks that mediate innate immune function and neuronal synaptic plasticity, and prevents development of PIPN-related mechanical and cold hypersensitivities in non–tumor-bearing, T-cell–competent Sprague-Dawley rats.[8] Genetic studies of SCS[9,10] suggest that SCS also modulates macrophages, and the effects may vary on the basis of parameters and timing of SCS (preemptive, early, or late to pain development) and etiology of the pain condition. However, these previous studies did not investigate whether SCS-induced macrophage modulation could act systemically to alter chemoefficacy and tumor growth.

Potential off-target effects on tumor growth are an essential consideration when developing CIPN therapeutics. Nevertheless, SCS continues to be used for non-CIPN pain treatment in patients with cancer and survivors of cancer despite its unknown effects on chemoefficacy, tumor growth, or recurrence.[11] To address this knowledge gap, we developed a xenograft model of NSCLC using a luciferase-expressing human NSCLC cell line in a T-cell–deficient

rat strain (Crl:NIH-*Foxn1*^{rnu}), also known as Rowlette Nude (RNU) rats that have been commonly used to examine tumor growth. RNU rats have a normal composition of B cells and an elevated number of natural killer (NK) 1 (NK and NK T) cells, which have been implicated in pain development.[12] We used reflexive pain behaviors and locomotor assays, in vivo bioluminescent imaging, Western blot, multiplex immunoassay, and immunohistochemistry to examine tumor growth and neuroimmune mediators of pain development after preemptive SCS (during PTX treatment) and late SCS (after PTX treatment) in this novel tumor-bearing CIPN and SCS model. Our study may be the longest SCS study (six weeks) conducted in animals to study the long-term effects of SCS on CIPN. We hypothesized that SCS can prevent CIPN pain and enhance chemoefficacy partially by modulating macrophages, fractalkine (CX3CL1), and inflammatory cytokines.

MATERIALS AND METHODS

Animals

Adult male rats (n = 88; 225–275 g starting weight;Crl:NIH-RNU; Charles River Laboratories, Wilmington, MA) were allowed to acclimate for a minimum of 48 hours before any experimental procedure. The rats were housed separately after SCS electrode implantation and were given access to food and water ad libitum. Our selection of RNU rats is based on previous characterizations of neuropathic pain and tumor growth in rats,[13,14] and on our experience with tumor growth and PTX-induced pain-related behaviors in this rat strain. All procedures involving animals were reviewed and approved by the Johns Hopkins Animal Care and Use Committee and were performed in accordance with the *NIH Guide for the Care and Use of Laboratory Animals*.

Group Allocation and Experimental Timeline

Rats were randomized to one of six groups: 1) no treatment (naïve, n = 16); 2) tumor only (tumor; n = 8); 3) PTX only (PTX; n = 8); 4) PTX with tumor (PTX + tumor; n = 16); 5) sham SCS with PTX and tumor (sham SCS + PTX + tumor; n = 20); and 6) active SCS with PTX and tumor (SCS + PTX + tumor; n = 20) (Fig. 1). Baseline pain behaviors were assessed in all animals before experimental procedures. Rats were implanted with SCS electrodes (groups 5 and 6) and/or tumor cells (groups 2, 4–6) at week 0. A 2 mg/kg PTX treatment (groups 3–6) was administered intraperitoneally every other day during week 2 for a cumulative PTX dose of 8 mg/kg (Supplementary Data), and SCS or sham SCS (groups 5 and 6, respectively) was applied during weeks 2 and 4. All rats that completed all group-assigned procedures appeared healthy and were included in all analyses. For tumor imaging and behavioral experiments, data from animals that had severe health problems during the experiments were excluded. To also study the more independent effects of SCS on tumor growth, SCS was not performed during week 3 to allow a wash-out interval beyond five half-lives of PTX (one half-life < 24 hours[15]). All animals were euthanized by overdose of isoflurane by week 6, and the L4–L5 DRG and tumors were harvested, and flash frozen on dry ice.

Human NSCLC Cell Line

Cancer cells were derived from a luciferase-expressing human NSCLC cell line. The A549-Luc2 cell line [Organism: Homo sapiens, human (male Caucasian aged 58 years)/Cell Type: epithelial/Tissue: lung/Disease: Carcinoma) was obtained commercially from ATCC (ATCC® CCL-185-LUC2™). With a humidity incubator in an atmosphere of 5% CO2 at 37 °C, cells were cultured and expanded with Dulbecco's Modified Eagle Medium: Nutrient Mixture F-12 (DMEM/F12+10% FBS+10% antimycotic/antibiotic).

Xenograft Establishment and Tumor Size

A549-Luc2 cells were trypsinized, centrifuged, and counted. 1.0×10^6 cells/mL were resuspended in serum free media and mixed with Growth Factor Reduced Matrigel (Corning;Corning, NY) at a 2:1 ratio, to a final volume of 100 μL.[16] A 22-gauge needle was used to inject the 100 μl cell-matrigel mixture into the subcutaneous flank region of RNU rats (10^5 cells/animal). We performed in vivo bioluminescent imaging of these tumors weekly using the IVIS® Spectrum Xenogen 200 system (IVIS, PerkinElmer, Alameda, CA). We administered intraperitoneal D-luciferase potassium salt before imaging, and quantified bioluminescence with *Living Image* software (PerkinElmer).[17] At the conclusion of the study by week 6, we harvested the tumor from each rat. Tumor size was estimated weekly through in vivo bioluminescence. Tumor volumes were calculated from caliper measurements using the modified Hansen formula, which is commonly applied for xenograft tumor volume estimations with calipers: $\text{Volume}\,(\text{mm}^3) = \frac{1}{2}$ the longest tumor diameter×the shortest tumor diameter^2.[18]

Electrode Placement and SCS Application

Using a model of CIPN in freely moving rats, we implanted a miniaturized SCS electrode (Fig. 1) to deliver SCS during and after PTX treatment (weeks 2 and 4, six–eight hours per day). A sterile, quadripolar SCS electrode (Medtronic Inc, Minneapolis, MN) that mimics clinical SCS was placed at the dorsal spinal cord of each rat (Fig. 1), as described in previous studies, and validated in rats.[8,19] Briefly, with rats under isoflurane anesthesia, we performed a laminectomy at the T13 vertebral level and inserted the electrode epidurally in the rostral direction. The position of the electrode was adjusted so that the contacts were at the T13–L1 spinal cord level, which corresponds to the lower thoracic-upper lumbar region (Fig. 1). The paddle electrode was sutured to muscle to secure its position, and the proximal end was tunneled subcutaneously until it exited the animal at the top of its head for later connection to an external neurostimulator (Model 2100, A-M Systems, Sequim, WA). Rats that exhibited signs of spinal cord injury, poor lead placement, or damaged electrodes were euthanized and excluded from subsequent studies.

In twin-pairs SCS (Fig. 1), the first and third contacts of the lead from the rostral direction were set as anodes (+), and the second and fourth were set as cathodes (−). The paddle electrode has four contacts arranged 1 mm apart with a thickness < 0.25 mm to fit flat into the epidural space without causing cord compression or injury. Before SCS each day, the motor threshold for each animal was determined by slowly increasing the current amplitude from zero, until muscle contraction in the mid-lower trunk or hind limbs was observed in

response to 4 Hz stimulation at 0.2 milliseconds pulse width. Conventional SCS (50 Hz, 0.2 milliseconds, constant current, six–eight hours per session per day) was applied at an intensity that activated low-threshold A-fibers (80% motor threshold). Sham SCS occurred in the same environment, with the leads connected to the stimulator without transmission of any electric power.

Behavior, Locomotor Activity, and Motor Coordination

Mechanical hypersensitivity was measured with the up-down method by applying von Frey monofilaments to the midplantar surface of the hind paws, and paw withdrawal threshold was determined as previously described by using the Dixon method and formula (Supplementary Data).[20] The cold plantar assay was used to evaluate noxious cold sensitivity (Supplementary Data).[8] The Hargreaves plantar test was used to evaluate noxious heat sensitivity (Supplementary Data).[21] The open field test was used to assess the effect of CIPN and SCS on spontaneous locomotor activity (Supplementary Data). The rotarod test was performed to assess motor coordination (Supplementary Data).

Multiplex Assay and Western Blot of Rat DRG

A bead-based multiplex immunoassay, Bio-Plex Pro Rat Cytokine 23-Plex (catalog #12005641, Bio-rad, Hercules, CA), was used to determine pain-related cytokine and chemokine levels (Supplementary Data). This multiplex assay was more advantageous than traditional enzyme-linked immunoassay because it allowed the detection of multiple analytes simultaneously. We examined the amounts of soluble CX3CL1, CD68, and tumor necrosis factor (TNF)-α using Western blotting (Supplementary Data).

Immunostaining of Rat DRG

Dual chromogenic immune-labeling for CD68 and CX3CL1 was performed on formalin-fixed, paraffin-embedded sections of rat DRG (L4–L5) on a Ventana Discovery Ultra autostainer (Roche Diagnostics, Basel, Switzerland) (Supplementary Data). Stained slides were scanned using the Hamamatsu Nano Zoomer (Hamamatsu City, Japan) at 20× to 40× magnification. Analysis of rat DRG was performed using the digital imaging analysis platform, HALO™ 3.0 (Indica Labs, Albuquerque, NM), as described previously (Supplementary Data).[22]

Statistics

Statistical analysis was performed using GraphPad Prism (version 9.3.0, GraphPad Software, La Jolla, CA). All data showed a normal distribution. No outlier data were removed. Data are presented as mean ± SEM. A $p < 0.05$ was considered statistically significant. We used unpaired or paired two-tailed Student's *t*-tests for comparisons between two groups and one-way ANOVA with Bonferroni post hoc test for three or more groups at a single time point. When comparing among three or more groups at multiple time points, we used two-way ANOVA with Bonferroni post hoc test.

RESULTS

We developed a model of CIPN in freely moving male RNU rats implanted with a miniaturized SCS electrode (Fig. 1). PTX (2 mg/kg × four days) or vehicle was injected intraperitoneally two weeks after SCS electrode and tumor implantation. Rats received six to eight hours per day of SCS during weeks 2 and 4 (during and after PTX treatment) with conventional paresthesia-based waveform parameters (50 Hz, 0.2 milliseconds, 80% motor threshold). Reflexive pain behavior tests were performed weekly, and we also used bioluminescent imaging to monitor tumor growth weekly. Locomotor tests were performed before harvesting of lumbar DRG (L4–L5) at three weeks after the last PTX dose and one week after the last SCS treatment.

Behavior

SCS Prevents Development of PTX-Induced Mechanical Pain-Related Hypersensitivity in Rats—Compared with the naïve RNU rats, RNU rats in the PTX and PTX+Tumor groups had decreased paw withdrawal thresholds to mechanical stimuli after PTX administration, suggesting that mechanical hypersensitivity after PTX is not T-cell dependent (Fig. 2b). The presence of the tumor did not significantly affect paw withdrawal thresholds. Notably, mechanical thresholds in PTX+Tumor rats that received preemptive SCS resembled those of naïve rats for the duration of the study, whereas sham stimulation was associated with decreased paw withdrawal threshold starting at week 2 (Fig. 2a,b). Therefore, we determined that preemptive SCS prevented development of PTX-induced mechanical pain-related hypersensitivity in RNU rats.

SCS Prevents Development Of Tumor-Induced Cold Pain-Related Hypersensitivity in Rats—Unlike Sprague-Dawley rats,[8] RNU rats did not develop cold hypersensitivity after PTX treatment alone (Fig. 2c). However, RNU rats in the Tumor and PTX+Tumor groups exhibited significantly shorter paw withdrawal latency to cold, which peaked during weeks 4 to 6 (Fig. 2c). Of note, rats in the SCS+PTX+Tumor group exhibited significantly longer paw withdrawal latency to cold stimulation than did those in the sham SCS+PTX+Tumor groups (Fig. 2d). These findings suggest that presence of tumor was sufficient to induce cold hypersensitivity in RNU rats and that SCS reduced this hypersensitivity. PTX did induce heat hypersensitivity in RNU rats;however, this was not attenuated with SCS, and no differences in paw withdrawal latency were found between animals that received SCS and those that received sham SCS (Supplementary Data Fig. S1a).

Tumor, But Not SCS, Attenuates PTX-Induced Gross Locomotor Coordination Impairment in Rats—To assess the effects of SCS on mobility and coordination in RNU rats that received PTX with and without tumor, we tested all groups with the rotarod and open field. We found no difference among groups in total distance traveled in the open field test (Fig. 2e,f; Supplementary Data Fig. S1b). In the rotarod test, animals in the PTX group fell faster than did animals in the Tumor and PTX+Tumor groups (Fig. 2g). SCS did not improve performance over that of sham SCS (Fig. 2f,h).

SCS Increases PTX's Antitumor Efficacy in Rats With Xenograft Human NSCLC

SCS is currently administered clinically to patients with cancer and survivors of cancer for the treatment of pain. To determine whether SCS alters the antitumor efficacy of PTX, we prospectively assessed tumor growth weekly. In addition to preemptive SCS (during PTX treatment), we delivered a second week of SCS (ie, late SCS) (after PTX treatment) beginning at the start of week 4, when we expected the last PTX dose to be cleared from systemic circulation. As expected, RNU rats that received PTX showed decreased tumor size by week 5 compared with rats that did not receive PTX (Fig. 3a,b). Notably, when tumors were measured by caliper volume, we found that SCS further reduced tumor size by week 5 (Fig. 3c). As expected, rats that received PTX had lower body weights than those of the naïve control (Supplementary Data Fig. S1e). SCS further reduced body weights compared with sham SCS, which suggests that SCS may increase PTX-induced weight loss or independently induce weight loss;however, we did not observe any changes in body weight compared with the tumor-only group, which overall suggests that these body weight changes may be subtle (Fig. 3d). Nevertheless, possible mechanisms for SCS-induced weight loss include increased gastric motility via electrical stimulation of viscera, modulation of the enteric nervous system, and changes in autonomic function.[23] Although NSCLC tumor progression and body weight have been noted to have an inverse correlation,[24,25] it is possible that the changes we observed in tumor size may be due to corresponding changes in body weight. Finally, visual inspection of tumors on autopsy also revealed decreased tumor sizes associated with SCS (Fig. 3e). Collectively, these findings suggest that preemptive SCS improved the antitumor efficacy of PTX, as indicated by decreased growth of subcutaneous A549-Luc2 NSCLC in RNU rats, but late SCS (post-PTX) did not alter tumor growth.

SCS Alters Expression of CX3CL1, CD68, TNF-α, and Inflammatory Cytokines in Rat DRG

Several studies have suggested that macrophage activation induces pain via downstream interaction of proinflammatory mediators and nociceptive neurons.[6,7,26-28] Our group and others have identified marked effects of SCS treatment on immune pathways.[8-10] Therefore, we measured the overall expression and spatial distribution of macrophage and inflammation-related proteins in DRG to assess sensory neuron-associated macrophage infiltration and inflammation. We focused our examination of these processes on the specific effects of SCS in the context of PTX with tumor. These experiments were conducted by week 6 to investigate the role of these neuroimmune- and inflammation-related proteins in the (long-term) maintenance of CIPN pain and SCS-induced CIPN prevention.

SCS Increases Soluble CX3CL1, CD68, and TNF-α Expression and May Decrease Inflammation—Because inflammation is a key driver of neuropathic pain,[29] including CIPN[30], we performed a broad assessment of pro- and antiinflammatory cytokines and chemokines in lumbar DRG. SCS was associated with increased soluble CX3CL1, CD68, and TNF-α expression, compared with naïve and/or sham SCS control groups (Fig. 4a-c; Supplementary Data Fig. S2). Compared with naïve rats, the sham SCS+PTX+Tumor group showed decreased expression of the antiinflammatory cytokine interleukin (IL)-10 and increased expression of the proinflammatory cytokine RANTES, also known as CCL5, which suggests that PTX treatment in RNU rats with tumor may promote a proinflammatory environment (↓IL-10; ↑RANTES) in DRG (Fig. 4d). In contrast, the SCS+PTX+Tumor

group indicated decreased expression of the proinflammatory cytokines IL-18, -17A, and -12p70, compared with the naïve group (Fig. 4d; Supplementary Data Fig. S2). In addition, in comparison with the naïve group, SCS was associated with an increased antiinflammatory environment (↓IL-10; ↑IL-18, ↓IL-17A, ↓IL-12p70) and increased soluble CX3CL1, CD68, and TNF-?, which can be pro- or antiinflammatory depending on timing of expression and the concurrent local (eg, DRG) inflammatory milieu.

SCS Changes Neuronal and Nonneuronal CX3CL1 and CD68 Expression— To further examine sensory neuron-associated macrophage crosstalk, we measured the expression of insoluble CX3CL1, a chemokine isoform associated with neuron-macrophage adhesion, and CD68, a macrophage marker in the DRG harvested by week 6. CX3CL1 expression showed the greatest staining intensity in the perinuclear regions, varied considerably in the cytoplasm, and was occasionally observed along plasma membranes consistent with insoluble CX3CL1 (Fig. 5a). Perinuclear CX3CL1 likely indicates immature CX3CL1 that is present in the rough endoplasmic reticulum and endocytic vesicles before its transport and post-translational glycosylation steps.[31] Nonneuronal CX3CL1 immunostaining was most intense in satellite glial cells adjacent to neurons (Fig. 5a).

In contrast to the increase in soluble CX3CL1 expression after SCS, identified using Western blot (Fig. 4a), we found decreased insoluble CX3CL1 in DRG neurons and nonneuronal cells after SCS by immunostaining (Fig. 5b). SCS was associated with a greater proportion of CD68+ cells and decreased proximity between insoluble CX3CL1+ neurons and CD68+ cells (Fig. 5b). These findings suggest that SCS may increase soluble CX3CL1 (Fig. 4a) to promote chemotaxis of macrophages and decrease insoluble CX3CL1 expression in neurons (Fig. 5b), which may serve to limit the adhesion of macrophages to neurons.

DISCUSSION

We showed in a T-cell–deficient RNU rat model with xenograft human NSCLC that preemptive SCS (during PTX treatment) improved the antitumor efficacy of PTX. However, late SCS (after PTX treatment) did not alter tumor growth. We also showed that preemptive SCS may prevent development of CIPN pain. These findings correlate with our recent human report on the efficacy of early neuromodulation for acute herpes zoster and postherpetic neuralgia pain treatment and prevention in a patient with immunosuppression.[5] Mechanistically, our findings suggest that decreased insoluble CX3CL1 in neurons and nonneuronal cells and increased CD68+ macrophages in DRG may contribute to SCS-induced PIPN pain prevention. Furthermore, SCS may have increased chemoefficacy by inducing similar CX3CL1 changes systemically or by increasing perfusion and PTX delivery (Fig. 6).

Previous studies suggested that T cells may be involved in neuropathic pain, as observed through decreased pain with T-cell depletion.[42,43] However, our T-cell–deficient RNU rats with and without tumor showed robust mechanical and heat hypersensitivities after PTX administration, suggesting that a T-cell–deficient state does not prevent the initiation or maintenance of PIPN pain in rats. This finding is in line with other reports of non–T-cell–dependent neuropathic pain conditions, with and without IL-10 involvement.[44,45] However,

cold allodynia was not observed in PTX-treated RNU rats without NSCLC, and was also less pronounced in PTX-treated RNU rats with NSCLC than that in PTX-treated immunocompetent, nontumor-bearing Sprague-Dawley rats.[8] These findings suggest that cold hypersensitivity may be T-cell dependent, and that NSCLC may independently promote cold allodynia via unknown mechanisms. Furthermore, the ability of SCS to attenuate cold and heat hypersensitivities may be similarly T-cell dependent, as suggested by a recent work in which Aβ-fiber electrical stimulation differentially modulated spinal cord superficial dorsal horn neuron populations in a manner that was input and cell-type specific.[46]

Interestingly, locomotor coordination was only impaired in PTX-treated RNU rats without NSCLC. Similarly to the occurrence of sedative effects with opioids that develop in healthy individuals but not in those with severe pain,[47] the presence of tumor may mitigate PTX-induced locomotor impairment via a stimulatory effect. Previous studies suggested that the A549-Luc2 NSCLC secretome may contain mediators related to neuroprotection that help preserve locomotor coordination in RNU rats and counteract PTX-induced coordination impairment (eg, amyloidbeta [a peptide associated with Alzheimer's disease], insoluble CX3CL1,[48] and ADAM 10 [a protease that mediates neuroprotective cleavage]).[49]

SCS increased soluble CX3CL1 and decreased insoluble CX3CL1 in DRG neurons and nonneuronal cells, which may induce neuroprotection and partially contribute to the prevention of PIPN pain in RNU rats. Although CX3CL1 was reported to mediate CIPN pain in immunocompetent models,[26,28] other studies[50,51] suggested that specific isoforms of CX3CL1 could rather promote neuroprotection, repair, and inhibit pain development. For example, when insoluble, membrane-bound CX3CL1 is cleaved, the N-terminal fragment, soluble CX3CL1, is released and acts as a chemotactic signaling molecule that promotes migration of cells expressing the CX3CL1-receptor, primarily leukocytes.[31] This soluble form of CX3CL1 has been linked to neuroprotection after ischemic injury[52] and to neuronal recovery after excitotoxic insults.[51] The C-terminal fragment is later released intracellularly where it can translocate into the cell nucleus and modify gene expression by "back-signaling," which then can promote neurogenesis.[48] Neuronal expression of intracellular CX3CL1, similarly to our findings in rat DRG, has been reported to mediate macrophage recruitment and neuroprotection in HIV-1 encephalitis.[53]

Interestingly, SCS also increased TNF-α in rat DRG, which may promote soluble CX3CL1 production due to TNF-α-induced cleavage of CX3CL1.[54] Although TNF-α usually induces pain, in some circumstances, such as preemptive SCS, it may become neuroprotective by promoting increased release of soluble CX3CL1. The increase in soluble CX3CL1 and TNF-α after SCS may also be due to increased activity of shared cleavage enzymes, such as ADAM 10 and TNF-α-converting enzyme, also known as ADAM 17.[55] Thus, increased cleavage enzyme activity could be induced by SCS, directly or indirectly (eg, through SCS-induced antiinflammation in DRG).

SCS increased expression of CD68+ macrophages and their distance to CX3CL1+ neurons in DRG of PTX-treated RNU rats with tumor. This may be due to increased soluble CX3CL1, which promotes CD68+ macrophage chemotaxis, and decreased insoluble CX3CL1, which reduces sensory-neuron–macrophage adhesion.[56] This

would decrease adhesion and limit crosstalk between nociceptive sensory neurons and infiltrating macrophages in DRG, which normally initiate and maintain PIPN pain.[57] Thus, we speculate that preemptive SCS may prevent PIPN pain by promoting early macrophage recruitment via increased soluble CX3CL1, which, along with SCS-induced antiinflammation, promotes a neuroprotective macrophage phenotype (eg, M2 type).[34-37] In addition, repeated SCS treatments may decrease inflammation and pain hypersensitivity by increasing the expression of proresolving mediators such as resolving D1,[58] which upregulates antiinflammatory cytokines (eg, IL-10) and downregulates proinflammatory cytokines in macrophages [(eg, IL-17, a T-cell–independent contributor to PIPN pain)].[27]

Although CX3CL1 is sometimes associated with increased cancer cell proliferation and metastasis, others have found differential antitumor effects of soluble and insoluble forms of CX3CL1[38] and that increased CX3CL1 in the tumor microenvironment is associated with improved prognosis in colorectal, breast, and lung cancers, possibly owing to enhanced leukocyte migration, T-cell activation, and NK-cell–mediated cytotoxicity.[39-41] Our findings revealed that in addition to preventing CIPN pain, preemptive SCS enhanced the antitumor efficacy of PTX. Our finding that late SCS (after PTX treatment) did not alter tumor growth suggests that applying SCS for the treatment of established PIPN pain in patients with cancer and survivors of cancer may not affect tumor progression.

Increased chemoefficacy may result from increased drug delivery due to SCS-induced systemic vasodilation that increases peripheral (tumor) perfusion by alteration of sympathetic vasomotor activity[32] and/or peripheral release of calcitonin gene-related peptide that also decreases ischemic pain,[59,60] particularly in the presence of increased cytokine IL-10[61] and decreased inflammation[62] SCS has also been found to modulate DRG function via antidromic activation of large DRG neurons.[63] Relatedly, SCS is used in the clinic for treatment of pain and ischemia in patients with refractory angina and peripheral vascular ischemia.[33,64] Because the tumor implantation site was not within the sensory distribution of the DRG innervating the hind paws that were removed (L4, L5), we also speculate that SCS may decrease chemoresistance and xenograft human NSCLC cell proliferation by inducing systemic (including tumor microenvironment) CX3CL1 changes as seen in our rodent DRG. Alternatively, SCS may increase chemoefficacy via other tumor microenvironment alterations downstream to SCS-induced DRG CX3CL1 modulation, possibly through the previously mentioned leukocyte or NK-cell–mediated mechanisms.[38-41]

Recent work revealed a sex-specific neuroimmune contribution, particularly involving T cells, to neuropathic (eg, CIPN) and inflammatory pain conditions.[44,65] Future studies should include female rats, which would help examine potential sex-based dimorphism in CIPN pain and cancer response to SCS. Although we used the sham SCS group as a surrogate to be compared with the naïve group, future studies may examine the effects in rat groups with tumor and/or PTX alone. We acknowledge that PTX and SCS may result in “chronic” neuroimmune changes that may influence subsequent SCS effects on tumor growth. However, in accordance with our institutional Animal Care and Use Committee guidance to use the minimum number of animals, we applied a second week of SCS in the same animals after a wash-out interval (one week after the last PTX and SCS) beyond the half-life of PTX[15] and that used in SCS clinical trials.[66,67] Although we applied

a clinically common SCS waveform (ie, conventional tonic stimulation), alternate SCS waveforms (eg, high frequency, burst, subsensory), protocols (eg, intermittent, continuous, responsive), and application modalities (eg, extraspinal, intradural, temporary) may have differing mechanisms and effects on CIPN pain, chemoefficacy, and tumor growth.

CONCLUSIONS

Our findings suggest that SCS is a promising strategy to enhance chemoefficacy and prevent PIPN pain. Before applying SCS for cancer- and CIPN-pain treatment in the clinic, further studies are needed that incorporate other cancer-relevant CIPN models (eg, tumor-bearing, human biospecimen, and experimental) and chemotherapeutic regimens (eg, mono- or multi-agent cancer treatment strategies). An increased mechanistic understanding of SCS-induced modulation of CX3CL1+ cells and sensory-neuron–associated macrophages across rodents and patients with pain will help identify novel targets for new cancer and CIPN therapeutics.

Supplementary Material

Refer to Web version on PubMed Central for supplementary material.

Acknowledgements

The authors thank Sujayita Roy for technical assistance with immunohistochemistry (Oncology Tissue Services, Johns Hopkins University–School of Medicine, Baltimore, MD), Lei Zheng and Robert Anders for guidance on semiautomated immunohistochemistry image analyses (Zheng Laboratory, Anders Laboratory, and Tumor Microenvironment Laboratory, Johns Hopkins University–School of Medicine), Medtronic, Inc (Minneapolis, MN) for providing the electrodes for spinal cord stimulation, Tricia Niles and Worod Allak for technical assistance with multiplex immunoassay (Bloomberg Flow Cytometry and Immunology Core, Johns Hopkins University–School of Medicine), the Pain Research Core for facilitating the project (Blaustein Pain Research and Education Endowment and the Neurosurgery Pain Research Institute, Johns Hopkins University–School of Medicine), Elena Artemova and Desmond Jacob for technical assistance with in vivo tumor imaging (Miller Research Building Molecular Imaging Core, Johns Hopkins University), and for illustration, Tim Phelps © 2019 JHU AAM (Department of Art as Applied to Medicine, Johns Hopkins University–School of Medicine).

Source(s) of financial support:

This study was conducted at the Johns Hopkins University and supported by grants from the National Cancer Institute–National Institutes of Health (Bethesda, MD) CA255428 (Eellan Sivanesan);the Foundation of Anesthesia Education and Research (Eellan Sivanesan);the American Society of Regional Anesthesia and Pain Medicine (Eellan Sivanesan);the Blaustein Pain Education and Research Endowment (Eellan Sivanesan);and the Department of Anesthesiology and Critical Care Medicine, Johns Hopkins University–School of Medicine, Stimulating and Advancing ACCM Research Award (Eellan Sivanesan). This study was partially supported by grants from the National Institute of Neurological Disorders and Stroke (NINDS)—National Institutes of Health (NIH) (Bethesda, MD) NS110598 and NINDS–NIH NS117761 (Yun Guan). Funders had no role in study design, data collection, or data interpretation, or in the decision to submit the work for publication.

Data Availability

The data that support the findings of this study are available, upon reasonable request, from the corresponding author.

REFERENCES

1. Colvin LA. Chemotherapy-induced peripheral neuropathy: where are we now? Pain. 2019;160(suppl 1):S1–S10. [PubMed: 31008843]

2. Staff NP, Grisold A, Grisold W, Windebank AJ. Chemotherapy-induced peripheral neuropathy: a current review. Ann Neurol. 2017;81:772–781. [PubMed: 28486769]
3. Cata JP, Cordella JV, Burton AW, Hassenbusch SJ, Weng HR, Dougherty PM. Spinal cord stimulation relieves chemotherapy-induced pain: a clinical case report. J Pain Symptom Manage. 2004;27:72–78. [PubMed: 14711471]
4. Phan P, Khodavirdi A. Successful treatment of chemotherapy-induced peripheral neuropathy (CIPN) with spinal cord stimulation (SCS). Cancer Res. 2007;67(suppl 9):35.
5. Roybal AE, Sivanesan E, Chen Y. Case report: dorsal root ganglion (DRG) stimulation for acute neuropathic pain from acute herpes zoster infection. SAGE Open Med Case Rep. 2021;9:2050313X211062297.
6. Luo X, Huh Y, Bang S, et al. Macrophage toll-like receptor 9 contributes to chemotherapy-induced neuropathic pain in male mice. J Neurosci. 2019;39:6848–6864. [PubMed: 31270160]
7. Zhang H, Li Y, de Carvalho-Barbosa M, et al. Dorsal root ganglion infiltration by macrophages contributes to paclitaxel chemotherapy-induced peripheral neuropathy. J Pain. 2016;17:775–786. [PubMed: 26979998]
8. Sivanesan E, Stephens KE, Huang Q, et al. Spinal cord stimulation prevents paclitaxel-induced mechanical and cold hypersensitivity and modulates spinal gene expression in rats. Pain Rep. 2019;4:e785. [PubMed: 31875188]
9. Vallejo R, Gupta A, Kelley CA, et al. Effects of phase polarity and charge balance spinal cord stimulation on behavior and gene expression in a rat model of neuropathic pain. Neuromodulation. 2020;23:26–35. [PubMed: 31070863]
10. Stephens KE, Chen Z, Sivanesan E, et al. RNA-seq of spinal cord from nerve-injured rats after spinal cord stimulation. Mol Pain. 2018;14:1744806918817429. [PubMed: 30451078]
11. Crowther JE, Chen GH, Legler A, Gulati A. Spinal cord stimulation in the treatment of cancer pain: a retrospective review. Neuromodulation. 2022;25:693–699. [PubMed: 35410770]
12. Weisshaar CL, Winkelstein BA. Ablating spinal NK1-bearing neurons eliminates the development of pain and reduces spinal neuronal hyperexcitability and inflammation from mechanical joint injury in the rat. J Pain. 2014;15:378–386. [PubMed: 24389017]
13. Ho Kim S, Mo Chung J. An experimental model for peripheral neuropathy produced by segmental spinal nerve ligation in the rat. Pain. 1992;50:355–363. [PubMed: 1333581]
14. Hai J, Zhu CQ, Bandarchi B, et al. L1 cell adhesion molecule promotes tumorigenicity and metastatic potential in non-small cell lung cancer. Clin Cancer Res. 2012;18:1914–1924. [PubMed: 22307136]
15. Gao Y, Shen JK, Choy E, et al. Pharmacokinetics and tolerability of NSC23925b, a novel P-glycoprotein inhibitor: preclinical study in mice and rats. Sci Rep. 2016;6:25659. [PubMed: 27157103]
16. Sarabia-Estrada R, Ruiz-Valls A, Guerrero-Cazares H, et al. Metastatic human breast cancer to the spine produces mechanical hyperalgesia and gait deficits in rodents. Spine J. 2017;17:1325–1334. [PubMed: 28412561]
17. Aswendt M, Adamczak J, Couillard-Despres S, Hoehn M. Boosting bioluminescence neuroimaging: an optimized protocol for brain studies. PLoS One. 2013;8:e55662. [PubMed: 23405190]
18. Beh ST, Kuo YM, Chang W-SW, et al. Preventive hypothermia as a neuroprotective strategy for paclitaxel-induced peripheral neuropathy. Pain. 2019;160:1505–1521. [PubMed: 30839425]
19. Shechter R, Yang F, Xu Q, et al. Conventional and kilohertz-frequency spinal cord stimulation produces intensity- and frequency-dependent inhibition of mechanical hypersensitivity in a rat model of neuropathic pain. Anesthesiology. 2013;119:422–432. [PubMed: 23880991]
20. Dixon WJ. Efficient analysis of experimental observations. Annu Rev Pharmacol Toxicol. 1980;20:441–462. [PubMed: 7387124]
21. Cheah M, Fawcett JW, Andrews MR. Assessment of thermal pain sensation in rats and mice using the Hargreaves test. Bio Protoc. 2017;7:e2506.
22. Jurcak NR, Rucki AA, Muth S, et al. Axon guidance molecules promote perineural invasion and metastasis of orthotopic pancreatic tumors in mice. Gastroenterology. 2019;157:838–850.e6. [PubMed: 31163177]

23. Pereira E, Foster A. Appetite suppression and weight loss incidental to spinal cord stimulation for pain relief. Obes Surg. 2007;17:1272–1274. [PubMed: 18074506]
24. Lam VK, Bentzen SM, Mohindra P, et al. Obesity is associated with long-term improved survival in definitively treated locally advanced non-small cell lung cancer (NSCLC). Lung Cancer. 2017;104:52–57. [PubMed: 28213000]
25. Zhang X, Liu Y, Shao H, Zheng X. Obesity paradox in lung cancer prognosis: evolving biological insights and clinical implications. J Thorac Oncol. 2017;12:1478–1488. [PubMed: 28757418]
26. Old EA, Nadkarni S, Grist J, et al. Monocytes expressing CX3CR1 orchestrate the development of vincristine-induced pain. J Clin Invest. 2014;124:2023–2036. [PubMed: 24743146]
27. Luo X, Chen O, Wang Z, et al. IL-23/IL-17A/TRPV1 axis produces mechanical pain via macrophage-sensory neuron crosstalk in female mice. Neuron. 2021;109:2691–2706.e5. [PubMed: 34473953]
28. Huang ZZ, Li D, Liu CC, et al. CX3CL1-mediated macrophage activation contributed to paclitaxel-induced DRG neuronal apoptosis and painful peripheral neuropathy. Brain Behav Immun. 2014;40:155–165. [PubMed: 24681252]
29. Bang S, Xie YK, Zhang ZJ, Wang Z, Xu ZZ, Ji RR. GPR37 regulates macrophage phagocytosis and resolution of inflammatory pain. J Clin Invest. 2018;128:3568–3582. [PubMed: 30010619]
30. Chen O, Donnelly CR, Ji RR. Regulation of pain by neuro-immune interactions between macrophages and nociceptor sensory neurons. Curr Opin Neurobiol. 2020;62:17–25. [PubMed: 31809997]
31. Latchney LR, Fallon MA, Culp DJ, Gelbard HA, Dewhurst S. Immunohistochemical assessment of fractalkine, inflammatory cells, and human herpesvirus 7 in human salivary glands. J Histochem Cytochem. 2004;52:671–681. [PubMed: 15100244]
32. Linderoth B, Gunasekera L, Meyerson BA. Effects of sympathectomy on skin and muscle microcirculation during dorsal column stimulation: animal studies. Neurosurgery. 1991;29:874–879. [PubMed: 1758600]
33. Amann W, Berg P, Gersbach P, et al. Spinal cord stimulation in the treatment of non-reconstructable stable critical leg ischaemia: results of the European peripheral Vascular Disease Outcome Study (SCS-EPOS). Eur J Vasc Endovasc Surg. 2003;26:280–286. [PubMed: 14509891]
34. Ishida Y, Kimura A, Nosaka M, et al. Essential involvement of the CX3CL1-CX3CR1 axis in bleomycin-induced pulmonary fibrosis via regulation of fibrocyte and M2 macrophage migration. Sci Rep. 2017;7:1–12. [PubMed: 28127051]
35. Wang J, Pan H, Lin Z, et al. Neuroprotective effect of fractalkine on radiation-induced brain injury through promoting the M2 polarization of microglia. Mol Neurobiol. 2021;58:1074–1087. [PubMed: 33089423]
36. Panek CA, Ramos MV, Mejias MP, et al. Differential expression of the fractalkine chemokine receptor (CX3CR1) in human monocytes during differentiation. Cell Mol Immunol. 2015;12:669–680. [PubMed: 25502213]
37. Enam SF, Krieger JR, Saxena T, et al. Enrichment of endogenous fractalkine and anti-inflammatory cells via aptamer-functionalized hydrogels. Biomaterials. 2017;142:52–61. [PubMed: 28727998]
38. Vitale S, Cambien B, Karimdjee BF, et al. Tissue-specific differential antitumour effect of molecular forms of fractalkine in a mouse model of metastatic colon cancer. Gut. 2007;56:365–372. [PubMed: 16870716]
39. Conroy MJ, Lysaght J. CX3CL1 signaling in the tumor microenvironment. Adv Exp Med Biol. 2020;1231:1–12. [PubMed: 32060841]
40. Wege AK, Dreyer TF, Teoman A, Ortmann O, Brockhoff G, Bronger H. CX3CL1 overexpression prevents the formation of lung metastases in trastuzumab-treated MDA-MB-453-based humanized tumor mice (HTM). Cancers. 2021;13:2459. [PubMed: 34070094]
41. Dreyer TF, Kuhn S, Stange C, et al. The chemokine CX3CL1 improves trastuzumab efficacy in HER2 low–expressing cancer in vitro and in vivo. Cancer Immunol Res. 2021;9:779–789. [PubMed: 33906866]
42. Cao L, DeLeo JA. CNS-infiltrating CD4+ T lymphocytes contribute to murine spinal nerve transection-induced neuropathic pain. Eur J Immunol. 2008;38:448–458. [PubMed: 18196515]

43. Costigan M, Moss A, Latremoliere A, et al. T-cell infiltration and signaling in the adult dorsal spinal cord is a major contributor to neuropathic pain-like hypersensitivity. J Neurosci. 2009;29:14415–14422. [PubMed: 19923276]
44. Laumet G, Edralin JD, Dantzer R, Heijnen CJ, Kavelaars A. Cisplatin educates CD8+ T cells to prevent and resolve chemotherapy-induced peripheral neuropathy in mice. Pain. 2019;160:1459–1468. [PubMed: 30720585]
45. Krukowski K, Eijkelkamp N, Laumet G, et al. CD8+ T cells and endogenous IL-10 are required for resolution of chemotherapy-induced neuropathic pain. J Neurosci. 2016;36:11074–11083. [PubMed: 27798187]
46. Fan W, Sdrulla AD. Differential modulation of excitatory and inhibitory populations of superficial dorsal horn neurons in lumbar spinal cord by Aβ-fiber electrical stimulation. Pain. 2020;161:1650–1660. [PubMed: 32068665]
47. Jamison RN, Schein JR, Vallow S, Ascher S, Vorsanger GJ, Katz NP. Neuropsychological effects of long-term opioid use in chronic pain patients. J Pain Symptom Manage. 2003;26:913–921. [PubMed: 14527760]
48. Fan Q, Gayen M, Singh N, et al. The intracellular domain of CX3CL1 regulates adult neurogenesis and Alzheimer's amyloid pathology. J Exp Med. 2019;216:1891–1903. [PubMed: 31209068]
49. Dorandish S, Williams A, Atali S, et al. Regulation of amyloid-β levels by matrix metalloproteinase-2/9 (MMP2/9) in the media of lung cancer cells. Sci Rep. 2021;11:9708. [PubMed: 33958632]
50. Rosito M, Lauro C, Chece G, et al. Trasmembrane chemokines CX3CL1 and CXCL16 drive interplay between neurons, microglia and astrocytes to counteract pMCAO and excitotoxic neuronal death. Front Cell Neurosci. 2014;8:193. [PubMed: 25071451]
51. Trettel F, Di Castro MA, Limatola C. Chemokines: key molecules that orchestrate communication among neurons, microglia and astrocytes to preserve brain function. Neuroscience. 2020;439:230–240. [PubMed: 31376422]
52. Rosito M, Deflorio C, Limatola C, Trettel F. CXCL16 orchestrates adenosine A3 receptor and MCP-1/CCL2 activity to protect neurons from excitotoxic cell death in the CNS. J Neurosci. 2012;32:3154–3163. [PubMed: 22378888]
53. Tong N, Perry SW, Zhang Q, et al. Neuronal fractalkine expression in HIV-1 encephalitis: roles for macrophage recruitment and neuroprotection in the central nervous system. J Immunol. 2000;164:1333–1339. [PubMed: 10640747]
54. Hurst LA, Bunning RA, Sharrack B, Woodroofe MN. siRNA knockdown of ADAM-10, but not ADAM-17, significantly reduces fractalkine shedding following proinflammatory cytokine treatment in a human adult brain endothelial cell line. Neurosci Lett. 2012;521:52–56. [PubMed: 22641052]
55. Romera C, Hurtado O, Botella SH, et al. In vitro ischemic tolerance involves upregulation of glutamate transport partly mediated by the TACE/ADAM17-tumor necrosis factor-α pathway. J Neurosci. 2004;24:1350–1357. [PubMed: 14960606]
56. Kaur T, Zamani D, Tong L, et al. Fractalkine signaling regulates macrophage recruitment into the cochlea and promotes the survival of spiral ganglion neurons after selective hair cell lesion. J Neurosci. 2015;35:15050–15061. [PubMed: 26558776]
57. Yu X, Liu H, Hamel KA, et al. Dorsal root ganglion macrophages contribute to both the initiation and persistence of neuropathic pain. Nat Commun. 2020;11:264. [PubMed: 31937758]
58. Tao X, Luo X, Zhang T, Hershey B, Esteller R, Ji RR. Spinal cord stimulation attenuates mechanical allodynia and increases central resolvin D1 levels in rats with spared nerve injury. Front Physiol. 2021;12:687046. [PubMed: 34248674]
59. Croom JE, Foreman RD, Chandler MJ, Barron KW. Cutaneous vasodilation during dorsal column stimulation is mediated by dorsal roots and CGRP. Am J Physiol. 1997;272:H950–H957. [PubMed: 9124459]
60. Tanaka S, Barron KW, Chandler MJ, Linderoth B, Foreman RD. Low intensity spinal cord stimulation may induce cutaneous vasodilation via CGRP release. Brain Res. 2001;896:183–187. [PubMed: 11277991]

61. Baliu-Piqué M, Jusek G, Holzmann B. Neuroimmunological communication via CGRP promotes the development of a regulatory phenotype in TLR4-stimulated macrophages. Eur J Immunol. 2014;44:3708–3716. [PubMed: 25316186]

62. Jiang L, Zhang W, Li W, Ling C, Jiang M. Anti-inflammatory drug, leflunomide and its metabolite teriflunomide inhibit NSCLC proliferation in vivo and in vitro. Toxicol Lett. 2018;282:154–165. [PubMed: 29050931]

63. Linderoth B, Foreman RD. Conventional and novel spinal stimulation algorithms: hypothetical mechanisms of action and comments on outcomes. Neuromodulation. 2017;20:525–533. [PubMed: 28568898]

64. Foreman RD, Linderoth B, Ardell JL, et al. Modulation of intrinsic cardiac neurons by spinal cord stimulation: implications for its therapeutic use in angina pectoris. Cardiovasc Res. 2000;47:367–375. [PubMed: 10946073]

65. Singh SK, Krukowski K, Laumet GO, et al. CD8+ T cell-derived IL-13 increases macrophage IL-10 to resolve neuropathic pain. JCI Insight. 2022;7:e154194. [PubMed: 35260535]

66. Meier K, Nikolajsen L, Sørensen JC, Jensen TS. Effect of spinal cord stimulation on sensory characteristics: a randomized, blinded crossover study. Clin J Pain. 2015;31:384–392. [PubMed: 25119512]

67. Kriek N, Groeneweg JG, Stronks DL, De Ridder D, Huygen FJ. Preferred frequencies and waveforms for spinal cord stimulation in patients with complex regional pain syndrome: a multicentre, double-blind, randomized and placebo-controlled crossover trial. Eur J Pain. 2017;21:507–519. [PubMed: 27714945]

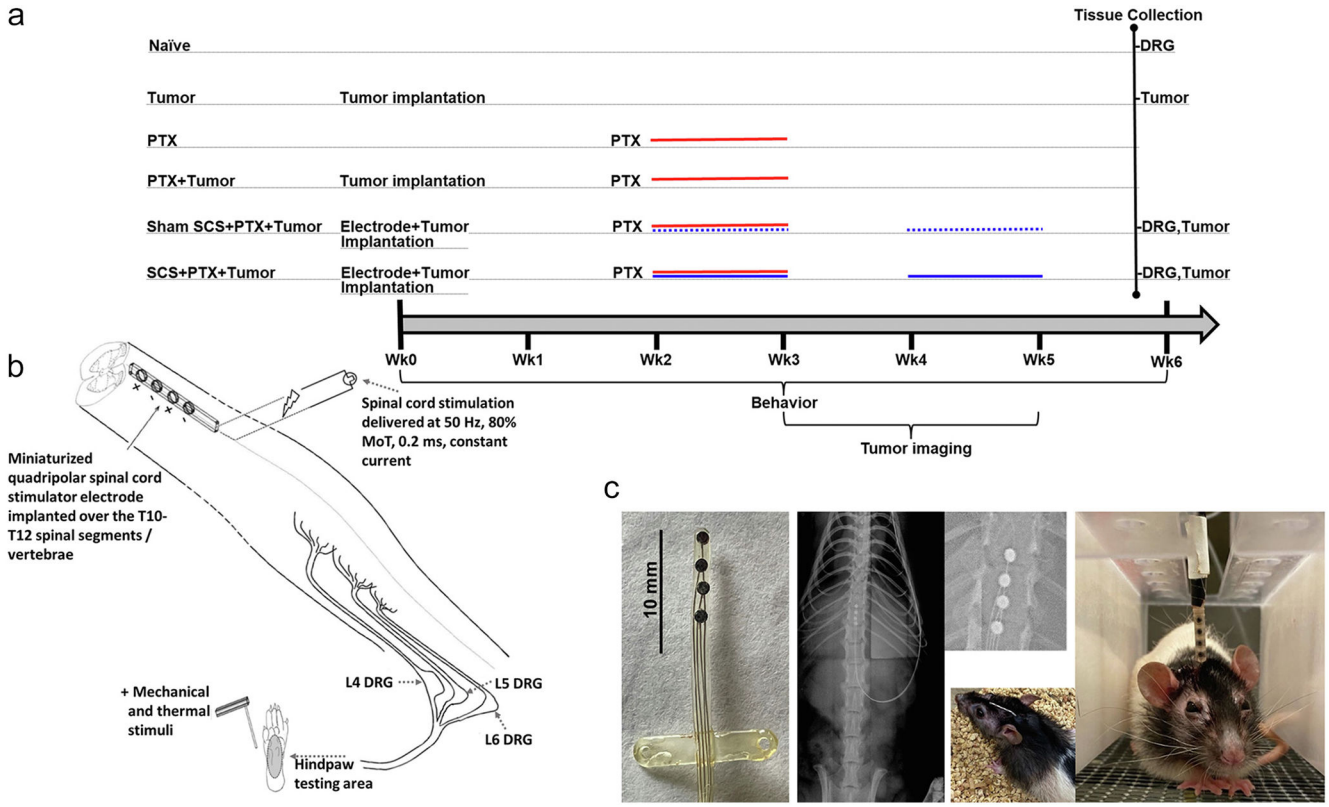

Figure 1.

Experimental protocol and schematic of SCS application. a. SCS electrode and tumor were implanted at week 0. PTX treatment during week 2 (red bars). Two periods of SCS were administered (blue bars). Preemptive SCS (during PTX treatment) was applied during week 2, and late SCS (after PTX treatment) was applied during week 4. Pain behavior assessments and in vivo bioluminescent tumor imaging occurred weekly. DRG and tumors were recovered by week 6. b. Schematic diagram illustrating the experimental setup for in vivo SCS application and pain behavior testing. c. Left: miniature quadripolar SCS electrode; middle: representative fluoroscopic images of SCS electrode after placement over T10–T12 vertebral level (~T13–L1 spinal levels). Right: freely moving (awake) RNU rat receiving SCS through an external stimulator connected to quad-electrode rings at the proximal end of SCS electrode (located near rat head).

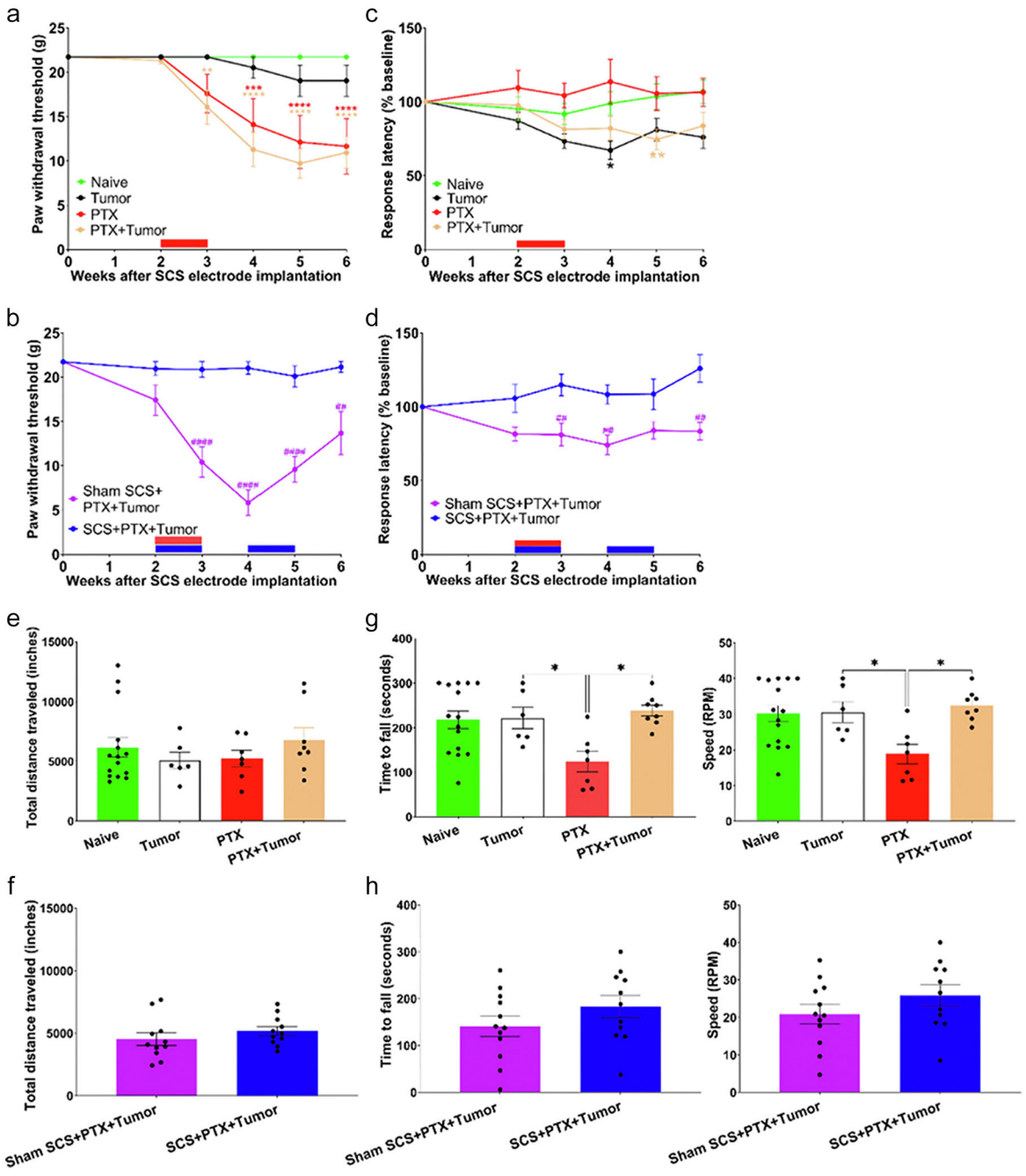

Figure 2.

Preemptive SCS (during PTX treatment) prevents PTX-induced pain-related mechanical hypersensitivity and partially attenuates cold hypersensitivity in rats. a and b. Changes in paw withdrawal threshold to mechanical stimuli (von Frey filaments), and (panels c and d) paw withdrawal latency to cold stimulation with dry ice. Red bars indicate the duration of PTX treatment. Blue bars indicate SCS application intervals. e and f. Total distance traveled in open field tests as an assessment of locomotor activity, and (panels g and h) measures of gross locomotor coordination from rotarod testing after PTX and SCS. Open field and rotarod testing were performed during week 3, one week after late SCS (after PTX

treatment). Two-way mixed-model ANOVA and Bonferroni's post hoc. Unpaired t-test with Welch's correction. *$p < 0.05$, **$p < 0.01$, ***$p < 0.001$, ****$p < 0.0001$ Naïve vs Tumor, PTX, or PTX+Tumor; (panels a and c) $n = 16$, $n = 8$, $n = 8$, $n = 16$; (panels e and g) $n = 15$, $n = 6$, $n = 7$, $n = 8$. ##$p < 0.01$, ####$p < 0.0001$ Sham SCS+PTX+Tumor vs SCS+PTX+tumor; (panels b and d) $n = 17$, $n = 18$; (panels f and h) $n = 11$, $n = 12$. Data represent mean ± SEM.

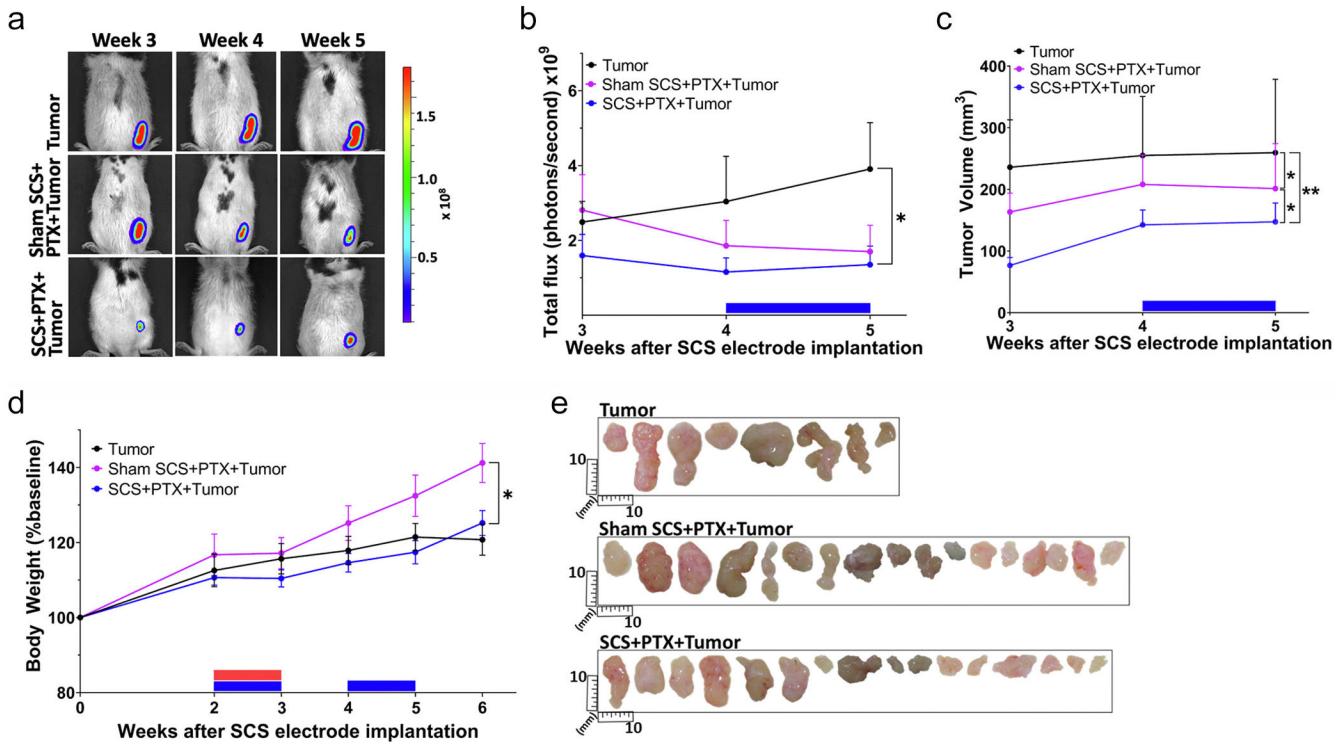

Figure 3.

Preemptive SCS (during PTX treatment) increases chemoefficacy, and late SCS (after PTX treatment) does not alter tumor growth. a. Representative serial in vivo bioluminescent images of xenograft NSCLC performed immediately after and in between each SCS application, in which red, green, and blue pixels represent high, mid, and low regions of tumor cell density [*radiance* = *p/sec/cm2/sr* (2)], respectively. b. Quantification of in vivo tumor bioluminescence. c. Tumor volume calculated from external caliper measurements. d. Changes in body weight of RNU rats at each week compared with their baseline weight. e. Photographs of tumors that remained palpable immediately before autopsy (scale bar = 10 mm). Red bars indicate duration of PTX treatment, and blue bars indicate SCS application intervals. b–d. One-way ANOVA and Bonferroni's post hoc. $*p < 0.05$, $**p < 0.01$ for comparison between the Tumor ($n = 8$), Sham SCS+PTX+Tumor ($n = 18$), and SCS+PTX+Tumor ($n = 17$) groups. Data represent mean ± SEM.

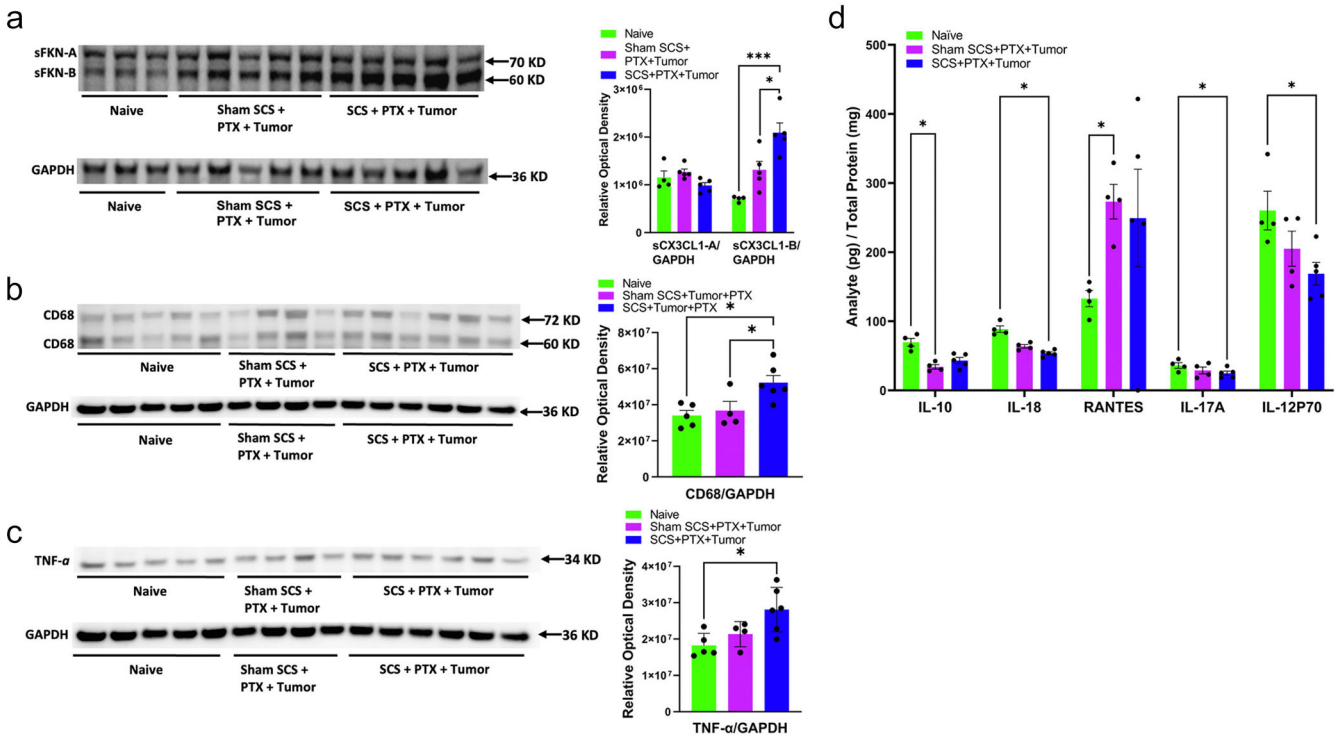

Figure 4.

SCS increased soluble CX3CL1, CD68, and TNF-α expression and may have decreased inflammation in DRG of rats. Western blot images (*left panels*), relative protein expression (*right panels*) of (panel a) soluble CX3CL1 (a chemokine that promotes migration of monocytes and macrophages), (panel b) CD68 (a heavily glycosylated macrophage and monocyte surface marker), and (panel c) TNF-α (a proinflammatory cytokine associated with soluble CX3CL1 release). d. Multiplex immunoassay expression levels of the antiinflammatory cytokine IL-10 and proinflammatory cytokines IL-18, -17A, -12p70, and RANTES, at one week after SCS. Naïve, Sham SCS+PTX+Tumor, SCS+Tumor+PTX; n = 4–6 rats/group. One-way ANOVA followed by Bonferonni's post hoc. *$p < 0.05$, ***$p < 0.001$, ****$p < 0.0001$. Data represent mean ± SEM. The images shown are cropped. The full-length original Western blot images are shown in Supplementary Data Figure S2.

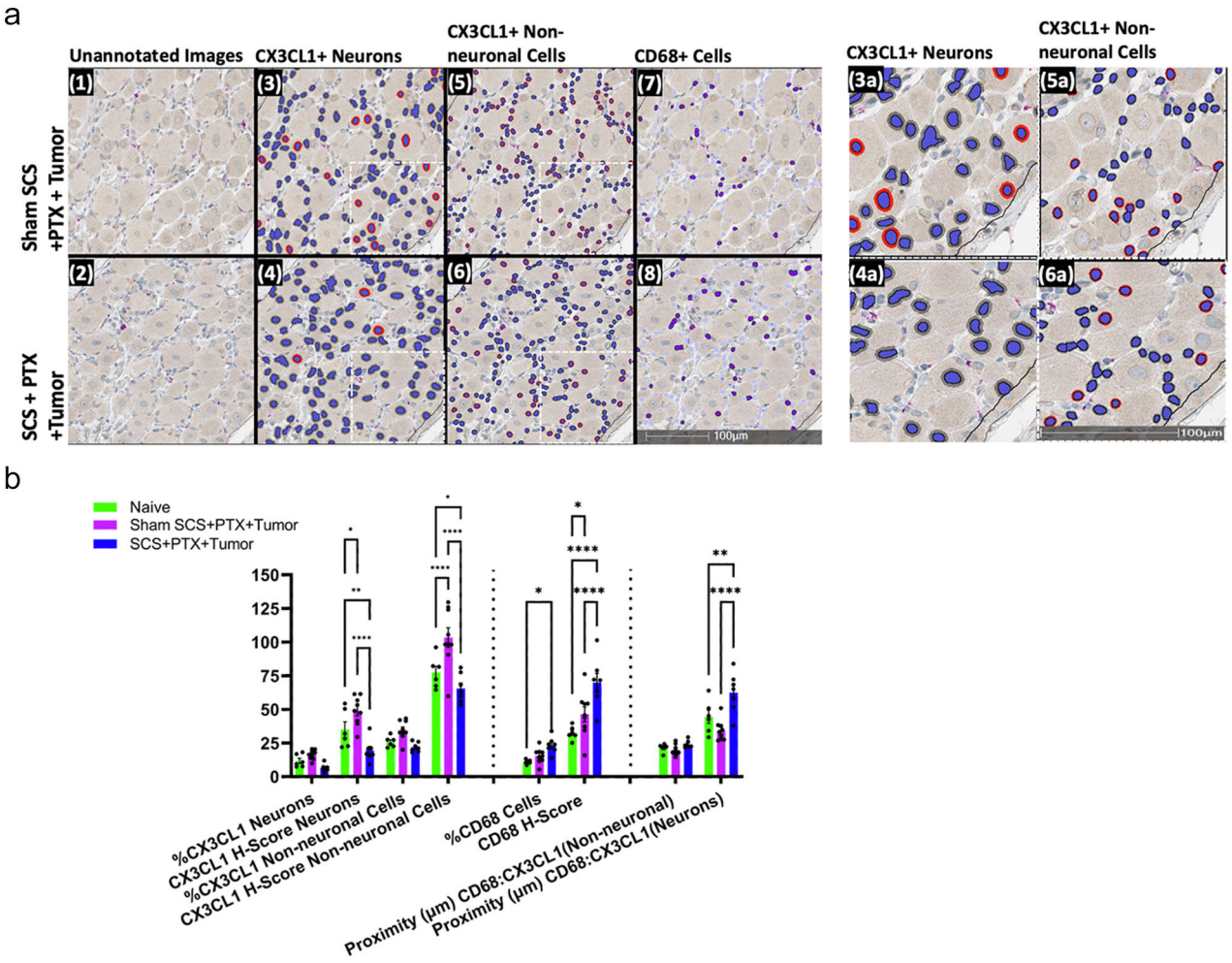

Figure 5.

SCS decreased insoluble CX3CL1 in neurons and nonneuronal cells but increased CD68+ macrophages in DRG of rats. a. Representative images of DRG from rats that received SCS or sham SCS. Paraffin sections were immunostained with CX3CL1 (DAB/brown) and CD68 (violet) and then counterstained with hematoxylin (blue) (parts 1–2). Images were imported into HALO™ software for automated measurement of CX3CL1 and CD68 staining (three right parts). Neuronal nuclei (parts 3–4) and nonneuronal (parts 5–6) nuclei are masked. Red overlay of these masked nuclei indicates CX3CL1+ staining. CD68+ cells are highlighted (parts 7–8). Higher magnification insets of masked neuronal nuclei and nonneuronal nuclei (parts 3a–6a). b. Quantification of immunostaining (panel a) and proximity of CD68+ cells to CX3CL1+ cells within 100 µm. Naïve, Sham SCS+PTX+Tumor, SCS+Tumor+PTX; n = 3 rats/group with two to three sections per rat (≈6–9 sections/group). One-way ANOVA followed by Bonferonni's post hoc. *$p < 0.05$, ***$p < 0.001$, ****$p < 0.0001$. Data represent mean ± SEM.

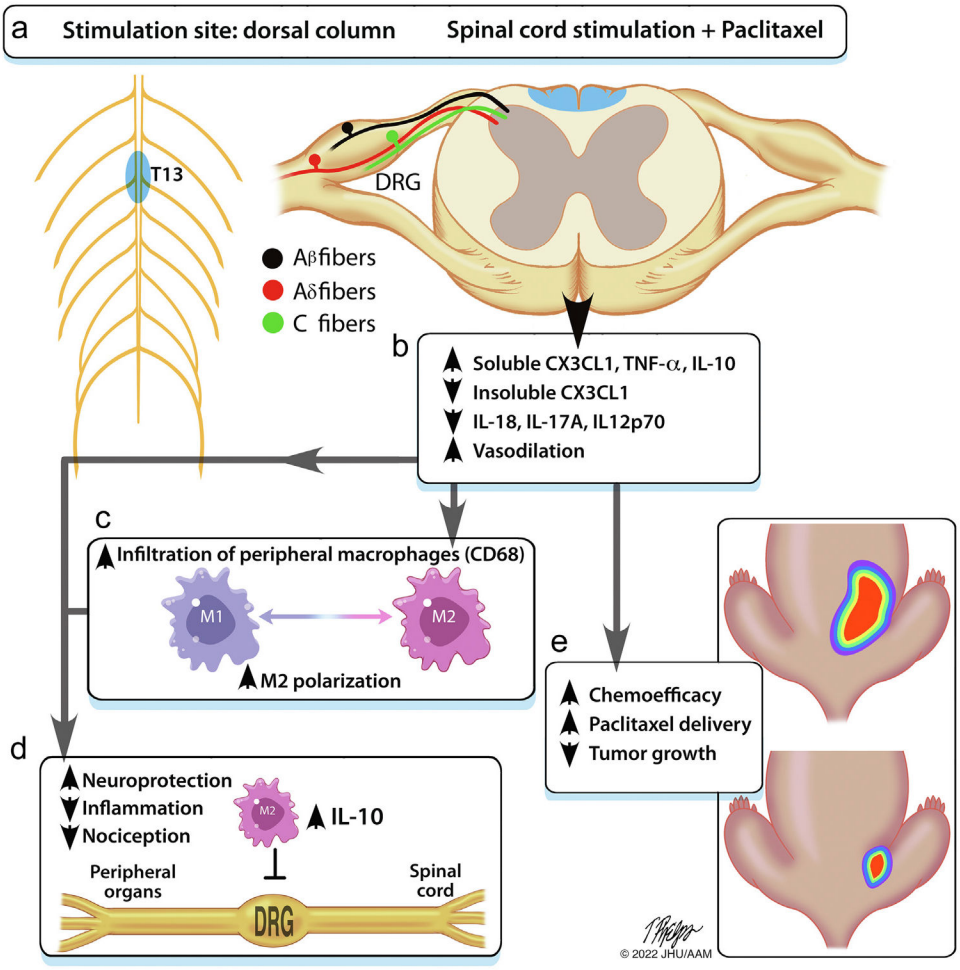

Figure 6.

Proposed model for the role of preemptive SCS in improving chemoefficacy and attenuating the development of CIPN pain. a. Dorsal column stimulation leads to (panel b) increased soluble CX3CL1, tumor necrosis factor-alpha (TNF-a), antiinflammatory cytokine IL-10, and vasodilation,[32,33] and decreased insoluble CX3CL1 and proinflammatory cytokines. c. Soluble CX3CL1 promotes chemotaxis of peripheral macrophages, which then undergo polarization[34-37] to (panel d) promote neuroprotection and decreased nociception. e. Modulation of CX3CL1 and vasodilation enhances chemoefficacy[38-41] and drug delivery to decrease tumor growth.